

FROM MEASUREMENTS TO MODEL: THE WALK ENGINE

Ronan Boulic, Pascal Glardon, Daniel Thalmann

Virtual Reality Lab, Swiss Federal Institute of Technology (EPFL), Lausanne, Switzerland

<mailto:{ronan.boulic, pascal.glardon, daniel.thalmann}@epfl.ch>

KEY WORDS: human motion, motion capture, virtual human, computer animation, virtual reality.

ABSTRACT

The present paper gives an overview of the modeling starting at the motion acquisition stage with an optical system and leading to a flexible real-time walk engine dedicated to the animation of autonomous virtual humans. First, we briefly describe how human motion acquisition process is done with a commercial optical system, stressing the remaining weaknesses regarding human motion measurements. We then recall the structure of the walking pattern that emerges from the findings of multiple biomechanics studies. In short, with proper normalization, time warping technique and mapping, it is possible produce on the fly a realistic walking pattern with continuously evolving velocity. Apart an intrinsic real-time requirement the described walking model addresses three issues: *generalization* (animation of a wide population of virtual humans for a wide range of the walking parameters), *openness* (user-defined personification of the gait style) and *reactivity* (changing the user defined context at any time while maintaining the coherence of the model).

1 INTRODUCTION

Human motion has always been difficult to simulate with acceptable level of physical realism and/or believability. It is especially the case when strong update rate requirements are imposed as in interaction context. Results from Neurophysiology suggest that many basic human skills could be seen as motion patterns managed at such low level as the spinal cord while the central brain is only in charge of modulating it according to the current context (Berthoz 02). Such findings are very stimulating for real-time human animation as relatively easy methods for motion capture are now available. Numerous approaches aiming at re-using and generalizing this raw motion material at low cost have been proposed (Rose & al. 98). Among them, statistical and probabilistic methods aim at encapsulating the structure of the motion implicitly, with only minimal normalization of the data (Brand & Hertzmann 00). Additional classification stages can map the motion database onto some high-level qualitative dimension. At the exploitation stage, specifying a value along that dimension leads to the low cost production of a new motion with the desired level of that qualitative property. The major limitation of this family of approaches comes from its black box nature and the unavoidable coupling between the various desired high-level qualities. Adding new samples to the motion database may improve some aspects while perturbing other dimensions.

An alternate computer animation technique is procedural modeling that strives for establishing explicit analytic formulation linking the high-level qualitative dimension to the animation parameters (i.e. the skeleton joint values). This is achieved through the careful analysis of numerous captured motion data reflecting faithfully the skill motion domain. In this paper, we concentrate on the walking motion due to its strategic importance in virtual human animation (Multon & al. 99); its pattern structure driven by only a small set of high-level parameters makes it an ideal case study for the methodology presented throughout this article. Other human actions featuring highly coordinated movements, like sitting on chairs of different heights, or reaching objects with a hand, are good candidates for this type of modeling.

Although this pattern presents strong spatial constraints on feet in the general context of curved locomotion, we show that a properly normalized direct kinematic model can provide an

approximation with a minimal foot sliding. Its low computing cost in the context of continuously evolving linear and angular velocities has made it the best compromise for populating large virtual spaces.

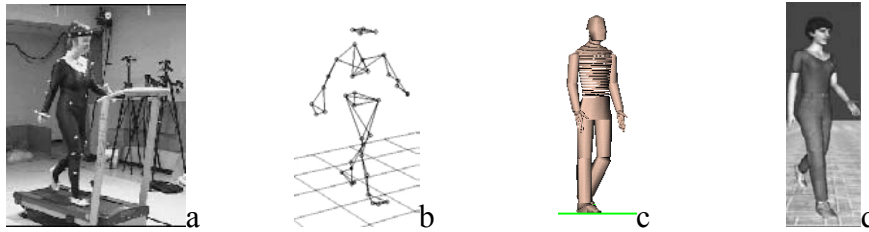


Figure 1: (a) Live motion capture session with 37 markers; (b) the result visualized in VICON™ BodyBuilder, (c) and (d) H-Anim compliant virtual humans animated by the walk engine.

We first describe the motion capture process as it is performed nowadays with a high-end commercial optical system, stressing the weaknesses remaining in the measurement chain from the marker positions to the joint angles (Menache 00) (Bodenheimer & al. 97). We then briefly recall the overall structure of the walking pattern as established from biomechanics studies (Boulic 90). Maintaining the coherence of the model while continuously changing the high-level parameters is an important issue that we tackle through geometric approaches for the feet sliding minimization in straight line. We then focus on the generalization to any human-like character compliant with the H-ANIM standard (Cobo & Bieri 02). We illustrate this issue through the mapping of the thorax-pelvis relative motion onto an anatomic spine model. Finally, we recall how to adapt the low level model to the characteristics of specific populations (Le 03) by extending to the Inman law.

2 HUMAN MOTION MEASUREMENT

2.1 Acquisition techniques

Presently the capture of full body human motion relies mostly on systems based on magnetic sensors, or on reflective markers seen by IR cameras. The magnetic system presents the disadvantages of covering a limited range of action and a high sensibility to metal that causes high distortions especially in the position data; its use is therefore limited to real-time interaction in situation where self-occlusion may often occur. On the other hand, optical motion capture systems offer a user-configurable active area depending on the number and the type of the cameras (e.g. VICON-8™ or BTS-ELITE™ systems). In the context of our current motion studies we prefer to use a treadmill to minimize the volume of the captured space. Presently, the eight infrared cameras ensure a viewed volume of $3 \times 2.5 \times 1.8 \text{ m}^3$. In this camera configuration, the absolute error on the position of a 25 mm diameter marker is 1mm. The cameras' hardware processes locally the IR-filtered image and sends the 2D coordinates of the viewed markers to a workstation responsible of the computation of the marker 3D position. The system used here is a commercial solution provided by *Vicon Motion System* and operating at 120 Hz (Vicon 03).

The motion capture volume has to be calibrated in two ways. First the static calibration is executed, by placing on the floor of the volume a L-bar on which markers are positioned at known distances. Then a dynamic calibration is made with another bar of known length also equipped with markers which are moved around the whole capture space. To capture motion, a subject wears stretch suits, where markers are positioned on them, at strategic locations (Figure 2).

The performance of the subject is then recorded, and the Vicon system reconstructs automatically the 3D markers from the 2D data acquired with the cameras. Only the 3D positions are exported from the system; this prevents the exploitation of a recent method merging the stage of 3D marker position reconstruction with the one of skeleton identification and motion mapping (Herda & al.

01). Instead, the 3D marker positions have to be cleaned from artefacts (phantom markers) or corrected by interpolating the holes in some occluded marker trajectories (Figure 3). Such cases happen when the subject exceeds the limits of the motion capture volume for example, or when reflecting objects (like the treadmill) are in the captured space.

The last stage is to label the markers correspondingly to a designed marker set that serves as the basis for computing the internal skeleton and the relative angles between consecutive segments (using the *Vicon BodyLanguage* programming language). For our purpose, we use a set composed of 37 markers, illustrated in Figure 3. Regarding the conventions of the skeleton modeling, we use the H-ANIM standard which defines a radical common denominator for the joints orientations (all the joints have the same orientation in the default posture) and a flexible topology for the hierarchical structure (any sub-set respecting the parent child relation is valid). These two key specifications aim at fostering the generalization of motion data (“design animation once, play on every compliant skeleton”). Section 3.2 comes back on the advantages of this approach.

To achieve the marker to joint angle mapping, we use a 3D Studio Max plug-in that needs as input parameters a marker position file and an HANIM skeleton.

The output file maintains the value of each joint transformation expressed as axis-angles. Depending on the joints, these transformations have one, two or three degrees of mobility in rotation. We will see in the next section that the walking pattern is better expressed in the major plane of motion, especially the sagittal plane of symmetry of the body (Figure 2b). For this reason, an Euler-angles formulation is preferred for defining the elementary walking trajectories but the final composition of the motion leads to the construction of quaternions for the animation of the H-Anim skeleton.

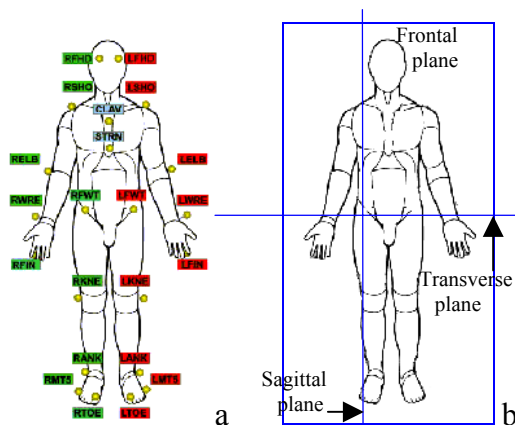


Figure 2: (a) Front view of the marker set used in Figure 1 (some markers are not visible) (b) Definition of the three anatomic planes: sagittal, frontal, transverse (adapted from Vicon tutorial)

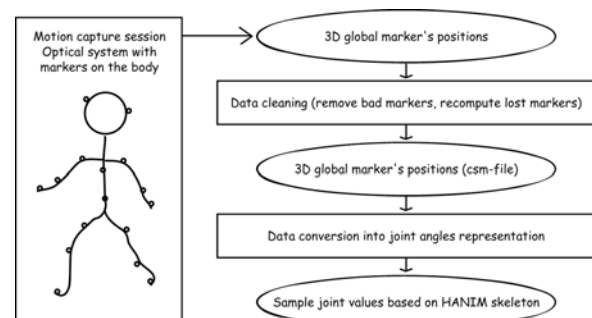


Figure 3: Human motion capture pipeline with a current high-end optical system.

2.2 Sources of errors in the conversion process

The process of converting the 3D marker positions into joint angles has two major sources of errors:

- In the *skeleton fitting* stage the joint centers and associated local frames are constructed using vectors built out of the markers' position in a reference pose or in a reference “gym” motion featuring all the degrees of mobility (Herda & al. 01). The strong assumption of a marker being rigidly linked to such a local frame biases the skeleton fitting and thus the deduced joint angles too. In (Herda & al. 01) the marker model allows a relative motion of the marker on a sphere centered on the joint. Marker movements are however more general (Boulic & al. 00). A systematic analysis of the local skin deformations as a function of all mobility parameters is needed to establish a complete marker model.

- The mechanical model of the skeleton is generally simplified with respect to Biomechanics to ease the design and the manipulation of motion. Secondary mobilities like small translations at the joint level are ignored thus introducing an error in the in the local position of markers. Here a joint model better reflecting anatomic shapes and deformations is needed to establish a more robust model of the relationship between the joint states and the skin deformation.

3 THE MODELING PROCESS

Despite its cost and remaining sources of errors, the motion capture process described above is the one offering the best compromise in term of precision nowadays. A measurement campaign targeting the identification of a given motion pattern would typically gather a subject population displaying a broad range of body sizes and morphotypes but a rather homogeneous age distribution (among the child / adult / elderly groups) as the age parameter is generally expected to induce large variation of the pattern (Le & al. 03). For our walk pattern modeling we have exploited walking data of adult men captured with video in major biomechanics studies (Murray 67). The purpose of these studies was to establish a pattern of normal walk in order to assess how some pathologies were affecting this pattern. For this reason the question of finding a normalization for which the pattern is the same for the whole population is essential. This is recalled in the next sections.

3.1 Structure of the walking pattern

The main interest of a normalized walking pattern is its genericity. Murray has shown that all the leg relative angles in the sagittal plane (hip, knee, ankle) were showing very similar trajectories for all adult men for the same value of the *normalized velocity* V obtained by dividing the walking velocity v (in m/s) by the Hip joint height H_t (i.e. the leg length in m), see Equation (1).

A generic straight-line walking pattern has been proposed with the local translation and the angular trajectories expressed as functions of a phase variable φ over a $[0,1]$ interval and parameterized by the normalized velocity (all trajectories are detailed in the appendix of (Boulic & al. 90)).

Due to the limitation in the measurement techniques, some angles represents a group of joints like for the relative orientation of the thorax with respect to the pelvis in the three anatomic planes (see section 3.3). The second major normalization aspect links the pattern normalized cycle to the time dimension through the Inman law that encapsulates the relationship between the cycle frequency f (a cycle is two steps) and the normalized velocity V (Inman & al. 81), defined in Equation (2).

We handle the time warp induced by a continuously varying velocity by integrating the frequency f over time (Boulic 90). In short, the phase variation $\Delta\varphi$ for a given duration Δt is given by Equation (3), where f is obtained from the instantaneous velocity through (2). An overview of the data flow for the update of the walking trajectories is shown on Figure 4. The next section describes how the pattern can be made even more generic with the H-Anim proposal.

$$V = \frac{v}{H_t} \quad f = 0.743 \cdot \sqrt{V} \quad \Delta\varphi = f \cdot \Delta t$$

Equations (1), (2), (3): Walking pattern time warping

3.2 The H-ANIM standard skeleton

The H-Anim proposal aims at fostering motion re-use through common conventions for human-like creatures (H-Anim) (Cobo & Bieri 02). Among its major conventions are a set of standardized joint names, an associated topology, and a frame orientation for all joints in the default posture.

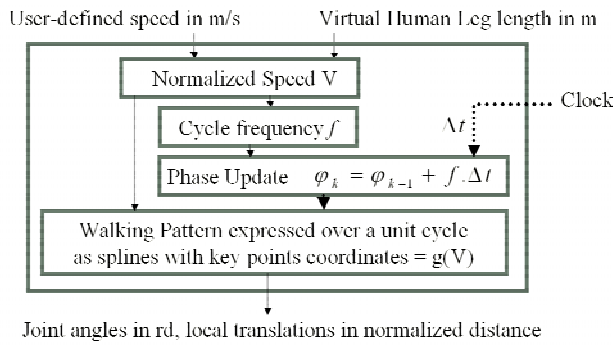


Figure 4: Use of the user-defined speed for the update of the walking trajectories

User-defined *desired speed* and *desired go-through position*

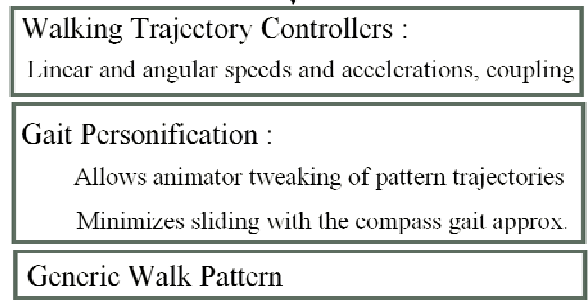


Figure 5: Three layers structure of the walk engine

3.3 The spine model and approximated mapping

One important convention in H-Anim is: “Any skeleton built as a subset of the H-Anim topology is H-Anim compliant”. As a consequent of the wide range of possible topologies, a dedicated layer has to map the walk engine trajectories (expressed as Euler angles in the anatomic planes) on the existing joints of any H-Anim compliant character. This is especially critical for the spine region. For this reason we have devised a simple algorithm that can be exploited for the mapping of other qualitative movements on an H-Anim spine.

At initialization time, we first count the number of vertebrae per spine regions (from pelvis to head: the lumbar, thoracic and cervical regions). Then during on-line animation the torso to pelvis relative orientation is first decomposed into a sequence of Euler angles acting in the three anatomic planes (tilt in the sagittal plane, roll in the frontal plane, torsion in the transverse plane). Then each Euler

	Forward-backward tilt	Lateral roll	Vertical torsion
skullbase			
vc1			
vc2			
vc3			
vc4			
vc5			
vc6			
vc7			
vt1			
vt2			
vt3			
vt4			
vt5			
vt6			
vt7			
vt8			
vt9			
vt10			
vt11			
vt12			
v11			null
v12			
v13			
v14			
v15			

Table 2: Anatomic model of spine showing the type of mobility distribution for the three spine regions (from bottom to top: lumbar, thoracic, cervical)

Uniform distribution	$C_i = \frac{1}{n}$
Linearly increasing	$C_i = i \cdot \left(\frac{2}{n \cdot (n+1)}\right)$
Linearly decreasing	$C_i = (n+1-i) \cdot \left(\frac{2}{n \cdot (n+1)}\right)$

Table 1: Expressions of the coefficients depending on the type of mobility distribution

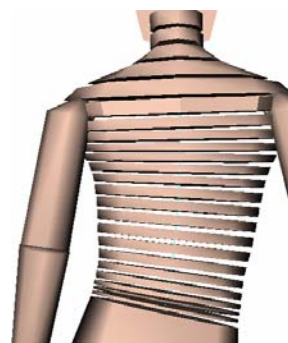


Figure 6: Spine mapping on a model with full spine

angle is distributed over a region of vertebrae according to a simplified anatomical model we built from reference data in (White & Penjabi 90). The coefficients from the distribution depend on the distribution type (uniform, linearly increasing, linearly decreasing) and on the number of available vertebrae n for a given spine region. Table 1 gives the expression of the distribution coefficients depending on the distribution type. Finally, the transformation associated to each vertebra is constructed by composing the three Euler angles contributions.

Although this method does not guarantee the exact reconstruction of the relative orientation defined by the walking model, it is sufficient from a qualitative point of view as the coherence of walk pattern is respected. The same process is applied for the desired head to torso relative orientation (Table 2). Figure 6 shows an example of mapping on the full spine

3.4 Basic personification of the walking pattern

By construction the walking trajectories reflect the average motion of adult men thus definitely lacking expressivity. However our end-user wants to be able to populate large virtual spaces with autonomous virtual humans that look like *living* there: we have to be able to convey *emotion through motion*. We have to provide a means to depart from the “average” model while retaining its qualities of coherence and natural flow of movement.

For this reason, the walk engine includes two layers on top of the walking pattern layer presented in the previous sections. These layers are (Figure 5):

- The Gait Personification (developed here)
- The Walking Trajectory Controllers

The Gait Personification layer allows the end-user to tweak the walking pattern with two parameters per dimension of the model: a scalar parameter cx and an offset parameter co using the following affine transformation:

$$Personified\ motion = cx * original\ motion + co \quad (4)$$

3.5 Ensuring the coherence of the model

The walking pattern is exploited as a direct kinematics model without trying to correct small potential feet misplacements. In fact the motion is more believable without Inverse Kinematics corrections because simplistic analytic correction methods destroy the natural dynamics of the motion pattern. On the other hand, more effective correction methods are either off-line or are not compatible with real-time requirements (we target crowd simulation).

The coherence between the three main variables (speed, step length and step frequency) is however ensured with the compass gait approximation (Figure 7). The Gait Personification layer is responsible of this task as the user tweaking of the *hip flexion-extension* trajectory through equation (4) might induce sliding artefacts. We consider only the hip flexion-extension trajectory in our coherence enforcement mechanism because it is the major determinant of the gait: it defines the step length at the beginning of the cycle. Our approach is to search for a normalized speed V_{hip} that produces a step length and a step frequency so that their product is the user-defined speed V_u .

Given the compass angle α between the legs at heel strike, the normalized step length S is defined as $S = 2.a \sin(\alpha/2)$. Then V_{hip} is such that the resulting S_{hip} and f_{hip} satisfy the user-defined speed $V_u = 2.S_{hip} \cdot f_{hip}$

One important consequence of this mechanism regarding the gait personification is the following: when the hip flexion trajectory is scaled down then the step frequency increases to ensure the user-defined speed (and vice versa for scaling up). In this way it is possible to build alternate characteristics to the Inman law. For example, we have been able to represent more closely the timing pattern of elderly people as a function of the speed (Le 03) because they make more steps instead of increasing the step length for higher speed.

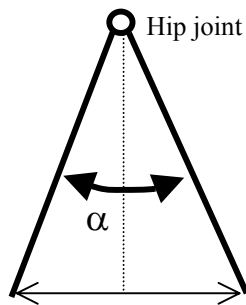


Figure 7: Compass gait, at heel strike, in the sagittal plane

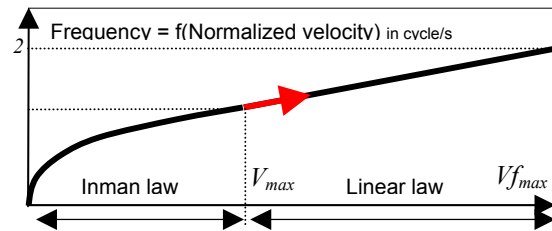


Figure 8: Extending Inman Law

4 EXTENSIONS OF THE MODEL

4.1 Extension of the Inman law

Equation (2) is valid until a maximum normalized velocity V_{max} for which the step length reaches its natural maximum value. Over that threshold, only the cycle frequency can be increased to produce a faster walking speed. This is achieved by extending the Inman law characteristic by a linear law with first order continuity (Figure 8). The current walking pattern is now able to handle normalized velocities up to a new maximum of 6 s^{-1} for a corresponding cycle frequency of 2 Hz. Although the corresponding gait style is closer to old news films than reality, the produced trajectories still retain the intrinsic smoothness of the initial walking pattern.



4.2 Key personification profiles

We have developed an interface allowing the definition of gait profiles where we can define key gait personification parameters for key linear velocity values (the whole set of scaling and offset coefficients is a bit less than 80 values). The gait personification parameters are linearly interpolated in-between the key speeds. Only a few of these values need to be changed to reflect the walking style of elderly persons (Le 03).

5 RESULTS

The results are live recorded animations from test applications running on top of VHD++ a middleware developed and VRLab and MIRAlab (Ponder & al. 03). Among numerous services it integrates the skinning service developed at MIRAlab (Cordier & al. 02). The animation files that can be found at the following web address: vrlab.epfl.ch/~boulic/WALK_Engine. Some of the animations were produced with a continuously changing context, like a desired velocity. The compass gait approximation limits the sliding effect of the walking motion. The following table highlights the specificity of two selected sequences.

Regarding the performances, all the live session recordings were made on a Pentium 4 1.7 GHz with a NVIDIA Quadro2 Pro graphic card.

 <p>Monsters</p>	<p>STRAIGHT_LINE : H-ANIM compliant characters differing by their size and proportions wrt to human proportions. Moving in straight line with linear velocity according to the Inman law and variations of it.</p>	 <p>Salami man</p>	<p>GAIT PERSONALITY: Extensive scaling and offset of the pattern. Extension of the Inman Law through the hip flexion scaling. Total number of spine joints to highlight pelvis to head anatomic mapping.</p>
---	---	---	---

6 DISCUSSION AND CONCLUSION

The important point worth mentioning in favor of the present model is the guarantee of providing a real-time walking animation for a wide range of characters, with personality, and a wide range of both linear and angular speeds.

Future work will concentrate on introducing additional parameters like the slope through motion capture measurements (some treadmills can have adjustable slope up to 12%). On the statistical side of the model, it will worth adding motion texture to make it more lively. In the longer term, we will explore on-line prediction of a few future steps for improving the adaptive control and the halting problem.

The monster model belongs to 3DS-Max Tutorial material. We wish to thank Mireille Clavien for the other characters and environment design, Michal Ponder for the VHD++ test application and support.

7 REFERENCES

- Berthoz A., *“Brain’s sens of motion”*, Harward University Press, 2002, also available in french in its original edition by Odile Jacob in 1996 under the title *“Le sens du mouvement”*.
- Bodenheimer, B., Rose, C., Rosenthal, S., Pella, J., *“The process of motion capture: Dealing with the data”*, Computer Animation and Simulation ’97, p. 3-18, 1997.
- Boulic R, Thalmann D, Magnenat-Thalmann N, *“A global human walking model with real time kinematic personification”*, The Visual Computer, Volume 6 (6), December 1990.
- Boulic R., Silaghi M.C., Thalmann D., *“Visualization of Local Movements for Optimal Marker Positioning”*, Proc. of AMDO’00, the ICPR’2000 Workshop on Articulated Motion and Deformable Objects, Palma de Mallorca, September 2000, Lecture Notes in Computer Science, Springer Verlag.
- Brand M., Hertzmann A., *“Style Machines”*, Proc. of SIGGRAPH’00, July 23-28, 2000, New Orleans, USA, and Technical Report TR-2000-14 MERL.
- Cobo M., Bieri H., *“Web3D Toolbox for creating H-Anim Compatible Actors”* Proc. of Computer Animation’02, p120-125, IEEE Press, ISBN0-7695-1594-0.
- Cordier F., Magnenat-Thalmann N., *“Real-Time Animation of Dressed Virtual Humans”*, Proc. of Eurographics’02, Saarbrücken.
- Herda L., Fua P., Plänkens R., Boulic R., Thalmann D., *“sing Skeleton-Based Tracking to Increase the Reliability of Optical Motion Capture”* Journal of Human Movement Science 20 (2001) 313-341.
- H-Anim: Humanoid Animation Working Group, www.hanim.org
- Inman VT, Ralston HJ, Todd F (1981) *“Human Walking”*, Baltimore, Williams & Wilkins.
- Le D.D., R. Boulic, D. Thalmann *“Integrating Age Attributes in a Virtual Human Locomotion Model”*, Proc. of int. Workshop on Visualization and Animation of Reality-based 3D Models”, ISPRS Commission V Working group 6, Tarasp-Vulpera, February 2003.
- Menache A., *“Understanding Motion Capture for Computer Animation and Video Games”*, ISBN 0-12-490630-3, Morgan Kaufmann, 2000.
- Multon F., France L., Cani-Gascuel M-P., Debunne G., *“Computer Animation of Human Walking : a Survey”*, J. Visual. Comput. Animat. 10, 39-54 (1999), J. Wiley&Sons.
- Murray M.P., *“Gait as a total pattern of movement”*, Am J Phys Med, Vol 46(1), 1967, pp 290-333.
- Ponder M., Herbelin B., Molet T., Schertenleib S., Ulicny B., Papagiannakis G., Magnenat-Thalmann N., Thalmann D., *“Immersive VR Decision Training: Telling Interactive Stories Featuring Advanced Virtual Human Simulation Technologies”*, Proceedings of Eurographics Workshop on Virtual Environments (EGVE), 2003.
- Rose C., Cohen M. F., Bodenheimer B., *“Verbs and Adverbs: Multidimensional Motion Interpolation”*, IEEE CGA September-October 1998 (Vol. 18, No. 5) pp. 32-40.
- Vicon-8 Motion Capture Sytem, www.vicon.com, 2003
- White A.A., Panjabi M.M., *“Clinical Biomechanics of the Spine”*, second edition, J.B. Lippincott Company, ISBN 0-397-50720-8, 1990.